The Asymmetric Nature of the Equatorial Undercurrent in the Pacific and Atlantic*

RUI XIN HUANG

Department of Physical Oceanography, Woods Hole Oceanographic Institution, Woods Hole, Massachusetts

FEI FEI JIN

Department of Meteorology, University of Hawaii at Manoa, Honolulu, Hawaii

(Manuscript received 10 October 2001, in final form 5 November 2002)

ABSTRACT

The structure of the Equatorial Undercurrent in a two-hemisphere ocean is studied, using a simple ideal-fluid model in which both potential vorticity and the Bernoulli function are conserved along streamlines. For the case of a symmetric forcing, the solution is reduced to the case discussed in previous studies. For the case of asymmetric forcing, the western boundary current from the hemisphere with stronger forcing overshoots the equator where the two western boundary currents merge and form an undercurrent that is asymmetric with respect to the equator. Layer thicknesses are continuous across the matching streamline, but zonal velocity can be discontinuous. Both the wind stress pattern and the Indonesian Throughflow are the most important factors dictating the asymmetric nature of the undercurrent.

1. Introduction

Mass communication from the subtropical ocean to the equator consists of two parts, that is, through the wind-driven circulation in the upper ocean and the deep meridional overturning cell of the thermohaline circulation. In this study we will focus primarily on the wind-driven circulation component of the mass communication. In the subtropical basin the wind-driven circulation can be further separated into two components: a poleward Ekman flux in the surface layer and a broad, subsurface, equatorward geostrophic flow driven by Ekman pumping. Such a partition is, however, impossible near the equator because the Coriolis parameter vanishes there and thus renders the Ekman layer meaningless.

Warm water subducted in the subtropical interior moves toward the equator in two ways, namely, through the low-latitude western boundary or through the interior communication window. These links have been identified through many observational studies. For example, Wyrtki and Kilonsky (1984) identified the source of the water mass in the equatorial current system using the Hawaii-to-Tahiti Shuttle Experiment; Gouriou and Toole (1993) studied the mean circulation of the upper layers of the western equatorial Pacific Ocean. These studies showed that the water mass in the equatorial current system comes from the subtropics. In particular, Gouriou and Toole (1993) pointed out that the water mass at the beginning of the undercurrent comes primarily from the Southern Hemisphere.

The interior communication window was also identified through tracer studies in 1970 and 1980. Fine and her colleagues (Fine et al. 1987; McPhaden and Fine 1988) have analyzed the tritium data and found a local tritium maximum around 140°W along the equator, which they rightly attributed to the ventilation of the subtropical water via subduction. Liu (1994) studied the interior communication associated with the circulation in the subtropical–tropical regime, using a ventilated thermocline model driven by zonally mean wind stress, and concluded that communication in the lower layer between the subtropics and Tropics is possible. On the other hand, McCreary and Lu (1994) and Lu and McCreary (1995) used a layered numerical model to study the influence of the ITCZ on flow between the subtropics and Tropics and estimated an interior communication rate of 3 Sv (Sv $\equiv 10^6$ m^3 s^{-1}) very close to an early estimate of 3 Sv across 10°N (Wijffels 1993).

Recent analysis of tracer and hydrographic data has led to a communication rate that is substantially higher. For example, Johnson and McPhaden (1999) estimated that this communication rate is about 5 Sv for the North Pacific and 16 Sv for the South Pacific. The communication rate in the Atlantic was estimated by Fratantoni

* Woods Hole Oceanographic Institution Contribution Number 10560.

Corresponding author address: Dr. R. X. Huang, Department of Physical Oceanography, Woods Hole Oceanographic Institution, Woods Hole, MA 02543.
E-mail: rhuang@whoi.edi

et al. (2000) as 1.8 Sv for the North Atlantic and 2.1 Sv for the South Atlantic. The mass flux through the interior communication window was discussed by Huang and Wang (2001), using a simple index based on the wind stress data only. This index can be used to illustrate the asymmetric nature of the interior communication between the Tropics and the subtropics. In addition, this index can be used to infer the decadal variability of the interior communication. However, this index cannot be used to infer the dynamical details of the equatorial currents.

Since the Coriolis parameter vanishes near the equator, geostrophy is inaccurate; thus, higher-order dynamics, such as the inertial terms and friction, are likely to be important. In a series of studies, Pedlosky (1987, 1996) has developed a theory for the dynamic connection between the subtropical thermocline and the Equatorial Undercurrent. The essence of the theory is that to lower order the Equatorial Undercurrent can be treated in terms of the ideal-fluid model. In order to conserve potential vorticity, the inertial term is retained near the equator.

Flow across the equator has been examined by many investigators—for example, Anderson and Moore (1979), Killworth (1991), and Edwards and Pedlosky (1998). Since the Coriolis parameter changes sign across the equator, it works as a potential vorticity barrier for cross-equatorial flow. Killworth showed that cross-equatorial flow is confined within a few deformation radii of the equator. In order to move beyond such a range, a frictional force is required to change the potential vorticity of the water parcels. The problem associated with frictional flow across the equator has been studied by many investigators, such as Edwards and Pedlosky (1998).

A further complication arises with the bifurcation of the western boundary currents. At low latitudes, the westward-flowing current bifurcates when it meets the western boundary, thus forming the poleward and equatorward western boundary currents. The best example is the northward Kuroshio and the equatorward Mindanao Current in the North Pacific. The bifurcation of the western boundary current involves complicated dynamics in three-dimensional space, including eddies and flow over complicated topography. However, a barotropic model may provide a simple solution that can be used as a crude estimate.

Our study is focused on the inertial theory of the undercurrent, so it may be considered as a further development of the inertial current theory. The model is formulated in section 2, where the undercurrent is treated in terms of a 2½-layer model with the inertial terms retained. As an example, the model is applied to the Pacific in section 3. With the asymmetric wind stress and the Indonesian Throughflow, the western boundary current from the Southern Hemisphere overshoots the equator and thus leads to some interesting structure in the undercurrent.

2. Model formulation

Throughout, we assume that the circulation is steady and can be treated in terms of an ideal-fluid model; thus both potential vorticity and the Bernoulli function are conserved along streamlines

$$\mathbf{u}_n \cdot \nabla q_n = 0; \qquad \mathbf{u}_n \cdot \nabla B_n = 0,$$

where the subscript n labels the layer. We make such assumptions for both the thermocline and the EUC (Equatorial Undercurrent) in the nature of a null hypothesis with regard to vertical mixing. That is, we attempt to see how much of the structure of the midlatitude and equatorial thermocline can be explained on the basis of the ideal-fluid theory. This is of course not the only legitimate point of view. Mixing does play an important role in the equatorial ocean. In addition, numerical experiments (e.g., Blanke and Raynaud 1997; Lu et al. 1998) require mixing for numerical reasons. The dynamic role of mixing (entrainment) was also explored through an analytical model (e.g., Pedlosky 1996). However, mixing seems to be of secondary importance in the source regime, that is, the western part of the Equatorial Undercurrent; hence we will use an ideal-fluid model to explore the dynamic structure in this study.

In the extratropics the potential vorticity can be approximated in terms of the planetary potential vorticity (i.e., $q_n = f/h_n$), while in the equatorial region the relative vorticity supplements the planetary vorticity. Since the strong currents there are zonal and very narrow, the semigeostrophic approximation leads to a representation of potential vorticity in the equatorial zone as $q_n = (f - \partial u_n/\partial_y)/h_n$. Similarly, the Bernoulli function in midlatitudes is given by the pressure field in each layer, which with the hydrostatic relation can be related to the layer thicknesses. In the equatorial region the pressure field is supplemented by the kinetic energy associated with the zonal velocity to form the Bernoulli function. The solutions in the two regions are joined together in a matching domain at the edge of the equatorial zone. The details of the dynamics in the individual regions were described by Luyten et al. (1983) and by Pedlosky (1996). Since the solution in the equatorial region must be computed numerically, the matching between the two regions is carried out at a latitude chosen to lie outside the EUC but close enough to the equator to represent the boundary layer character of the solution. The solution's character does not depend strongly on the latitude chosen for matching.

In the extratropics the structure of the thermocline is described in terms of a 2½-layer model of the ventilated thermocline. Assume the outcrop line is a zonal circle y_{out} where the Coriolis parameter is f_{out}. Poleward of the outcrop line there is only one moving layer, and the solution is well known. Since this part of the circulation is not our concern in this study, we omit the discussion

of it. Equatorward of the outcrop line there are two moving layers and the total layer depth, H_0, obeys

$$H_0^2 = \frac{D_0^2 + H_e^2}{1 + \frac{\gamma_1}{\gamma_2}\left(1 - \frac{f}{f_{\text{out}}}\right)^2}, \tag{1}$$

where

$$D_0^2(x, y) = -\frac{2f^2}{\gamma_2\beta}\int_{\lambda}^{\lambda_e} w_e r \cos\phi \, d\lambda', \tag{2}$$

γ_1 and γ_2 are reduced gravity across the upper and lower interfaces, $\beta = r^{-1}df/d\phi$, λ_e is the longitude of the eastern boundary, r is the radius of the earth, ϕ is latitude, and w_e is the Ekman pumping rate calculated from wind stress

$$w_e = \frac{1}{r\rho_0 2\Omega \sin\phi} \times \left(\frac{1}{\cos\phi}\frac{\partial\tau^{\phi}}{\partial\lambda} - \frac{\partial\tau^{\lambda}}{\partial\phi} + \frac{\tau^{\lambda}}{\sin\phi\cos\phi}\right), \tag{3}$$

where Ω is the angular velocity of earth's rotation; (τ^{λ}, τ^{ϕ}) are the zonal and meridional components of wind stress. For convenience, we will assume $\gamma_1 = \gamma_2 = 1$ cm s^{-2} and H_e is the total layer depth along the eastern boundary, and we set $H_e = 0$ in this study. The second assumption is used to avoid the complication introduced by the shadow zone; the dynamical role of the shadow zone is left for future study.

In the following analysis, we will use the basic scales for the equatorial motions (Pedlosky 1996):

$$l = \left(\frac{\gamma_2\tau_0 L}{\rho_0\beta^4}\right)^{1/8}, \quad H = \left(\frac{\tau_0 L}{\gamma_2\rho_0}\right)^{1/2}, \quad U = \left(\frac{\gamma_2\tau_0 L}{\rho_0}\right)^{1/4}. \tag{4}$$

The corresponding scale for the streamfunction is

$$\Psi = HUl.$$

Using these basic scales, the basic nondimensional variables are defined as

$$x = Lx', \quad y = ly', \quad h_1 = Hh_1', \quad h_2 = Hh_2', \quad u = Uu'. \tag{5}$$

For the Atlantic Ocean, $\tau_0 = 1$ dyn cm^{-2}, $\gamma_2 = 1.0$ cm s^{-2}, $\beta = 2 \times 10^{-13}$ cm^{-1} s^{-1}, $L = 3000$ km, so that $l = 256$ km, $H = 173$ m, $U = 1.32$ m s^{-1}, and $\Psi = 58 \times 10^6$ m^3 s^{-1}. For the Pacific Ocean, $L = 14\,000$ km so that $l = 310$ km, $H = 274$ m, $U = 1.93$ m s^{-1}, and $\Psi = 225 \times 10^6$ m^3 s^{-1}. These scales are close to the observed Equatorial Undercurrent in the oceans. Note that the undercurrent thickness is on the order of $0.1H$, so the volume flux contribution to the undercurrent from each hemisphere is on the order of 6 Sv for the Atlantic and 22 Sv for the Pacific.

In nondimensional form, the Coriolis parameter is $f = y$, and the wind stress is $\tau = \tau_0\tau'$. Since the matching latitude is very close to the equator, we can treat the wind stress as constant; that is, τ' is one unit. Thus, the layer thickness along the matching latitude is

$$H_0^2 = \frac{2(1 - x)}{1 + (1 - y_m/y_{\text{out}})^2}. \tag{6}$$

The corresponding thicknesses for the upper and lower layers are

$$h_1 = H_0(1 - y_m/y_{\text{out}}), \qquad h_2 = H_0 y_m/y_{\text{out}}. \tag{7}$$

The equatorial thermocline is described in terms of a two-moving-layer model (Pedlosky 1987, 1996). The major difference between the equatorial thermocline and the extratropical thermocline is that the Coriolis parameter vanishes near the equator; thus, geostrophy is no longer the dominating balance near the equator. Instead, the relative vorticity must play an important role in the dynamic balance of the Equatorial Undercurrent. Scaling analysis leads to a simple semigeostrophic model for the Equatorial Undercurrent and the thermocline. The equatorial thermocline can be described in terms of the total layer depth (h) and the zonal velocity in the second layer (u):

$$h_y = -yu \tag{8}$$

$$u_y = y - y_{\text{out}}\frac{h - h_1}{h + u^2/2}. \tag{9}$$

These balances assume that water flowing from the subtropics to the Tropics conserves both potential vorticity and Bernoulli function. The dependence of potential vorticity on the Bernoulli function, $h + u^2/2$, is determined by matching to the ventilated thermocline. This system of first-order differential equations is subject to the following boundary conditions: First, the lower interface depth should match that of the interior solution along the matching latitude y_m:

$$h = H_0 \quad \text{at } y = y_m. \tag{10}$$

Second, the equator is assumed to be a streamline so that the Bernoulli function should be a constant along the equator:

$$h + \frac{u^2}{2} = B_0 \quad \text{at } y = 0, \tag{11}$$

where B_0 is the Bernoulli function of the western boundary current at the bifurcation latitude, determined by the barotropic circulation in the subtropical basin interior controlled by the wind stress forcing. In the ocean interior the kinetic energy term $u^2/2$ is negligible compared with the layer thickness term h, so the Bernoulli function is reduced to $B = h$.

In this formulation, we implicitly assume that there is no mass flux through the western boundary of the basin, so the western boundary is a streamline. As we

will discussed in section 3, however, this assumption has to be modified for the Pacific because of the existence of the Indonesian Throughflow.

Note that the upper-layer thickness is another unknown. In order to carry out the boundary layer calculation, we also need to specify an additional constraint on the upper-layer thickness. Pedlosky (1987) first assumed that h_1 is independent of latitude within the equatorial boundary layer and found some interesting solutions. Another choice is to assume that the upper-layer thickness is compensated within the equatorial region (Pedlosky 1996). This choice is based on the following idea: the geostrophic velocity in the upper layer is much smaller than that in the second layer; thus, to the lowest-order approximation the meridional pressure gradient in the upper layer is negligible compared with that in the second layer. This approximation implies that near the equator the current in the upper layer is dominated by the local wind stress.

Of course this specification of the depth of the upper layer is entirely arbitrary. In the original theory as described by Pedlosky (1996) the two extremes of specification of the upper-layer thickness, that is, either independent of y with no vertical shear across the interface or completely compensated, had little effect on the undercurrent or the depth of the equatorial thermocline. In the interest of keeping our model as simple and comprehensible as possible, we retain this arbitrary and admittedly deficient element of the theory. Thus, we will use the following additional constraint on the upper-layer thickness:

$$h_1(x, y) = h_1(x, y_m) + h(x, y_m) - h(x, y), \quad (12)$$

where y_m is the latitude where the equatorial thermocline solution is matched with the interior thermocline solution. This is the compensated solution.

The equation set (8) and (9) plus boundary constraints (10), (11), and (12) constitute a boundary value problem of the two ordinary differential equations. As long as B_0 is specified, the solution can be found by a shooting method, as described by Huang and Pedlosky (2000).

A major assumption implicitly made in the model discussed above is that the solution is symmetric with respect to the equator. This implicit assumption does not hold exactly in real oceans. Due to the asymmetric nature of the atmospheric general circulation, wind stress near the equator is not symmetric. It is readily seen that a straightforward application of this model will lead to discontinuity of the solution for the equatorial thermocline.

A natural requirement is that the solution should be continuous across the equator. Thus, the minimum requirement is that the thickness of both the upper and lower layers should be continuous across the equator. Since the Bernoulli function carried by the corresponding western boundary currents in the two hemispheres is not the same, these two boundary currents should not match exactly along the equator. In other words, the matching latitude at each longitudinal section should be a free boundary determined from the interior dynamics.

Thus, the suitable boundary value problem for the branch originating from the Northern Hemisphere branch is

$$h^n = H_0^n \quad \text{at } y = y_m. \quad (13)$$

Second, the Bernoulli function should be a constant along the matching line near the equator:

$$h^n + \frac{u^2}{2} = B_0^n \quad \text{at } y = y_{\text{sep}}, \quad (14)$$

where B_0^n is the Bernoulli function of the western boundary current at the bifurcation latitude in the Northern Hemisphere, determined by the barotropic circulation in the subtropical basin interior. In addition, we will use the following additional constraint on the upper-layer thickness:

$$h_1^n(x, y) = h_1^n(x, y_m) + h^n(x, y_m) + \Delta h^{ns}\frac{y_m - y}{2y_m} - h^n(x, y), \quad (15)$$

where

$$\Delta h^{ns} = h_1^s(x, -y_m) + h^s(x, -y_m) - [h_1^n(x, y_m) + h^n(x, y_m)]$$

is the difference in the upper-layer pressure at the matching latitudes in the Northern and Southern Hemispheres.

The suitable boundary value problem for the branch originating from the Southern Hemisphere branch is

$$h^s = H_0^s \quad \text{at } y = -y_m. \quad (16)$$

Second, the Bernoulli function should be a constant along the matching line near the equator:

$$h^s + \frac{u^2}{2} = B_0^s \quad \text{at } y = y_{\text{sep}} \quad \text{and} \quad (17)$$

$$h_1^s(x, y) = h_1^s(x, -y_m) + h^s(x, -y_m) + \Delta h^{ns}\frac{y + y_m}{2y_m} - h^s(x, y). \quad (18)$$

Matching conditions (15) and (18) imply that pressure in the upper layer is continuous if these two boundary layers are matched at $y = 0$. Since the Bernoulli function plays a role similar to the pressure head, it is expected that the western boundary current that has the larger Bernoulli function should overshoot the equator and invade the other hemisphere, as shown in the sketch in Fig. 1a. In addition, there may be a small difference between the interior solution at the matching latitude in the two hemispheres; thus, there is a small pressure gradient in the upper layer, resulting from $\Delta h^{ns} \neq 0$. However, this may be a small contribution to the solution, so we will assume that $\Delta h^{ns} = 0$ for the following analysis.

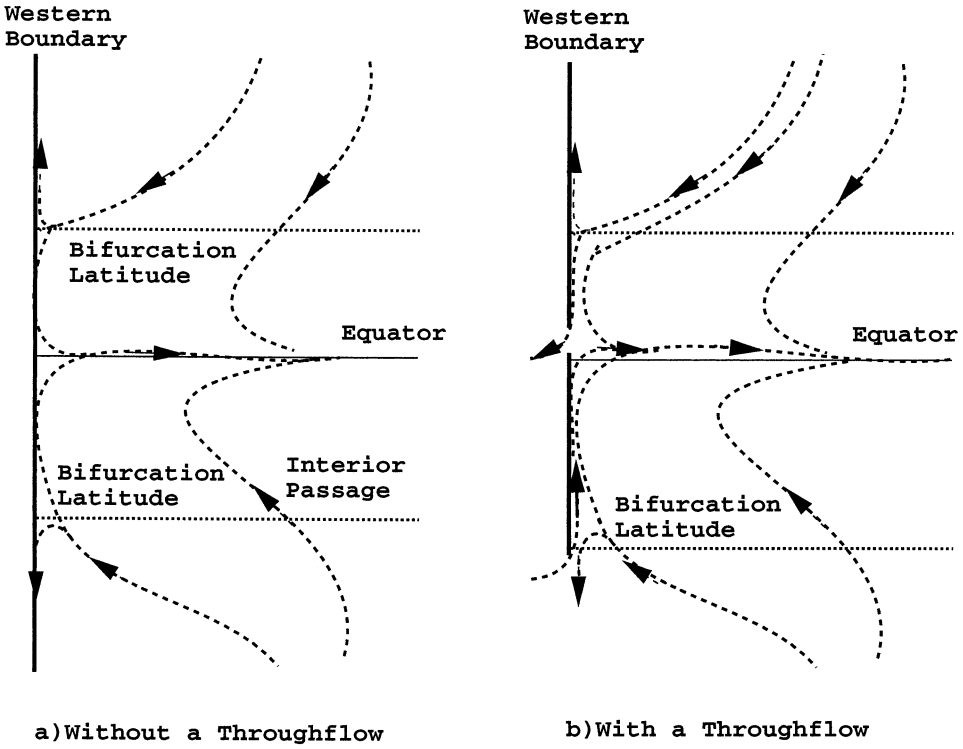

FIG. 1. Sketch of the Equatorial Undercurrent in a two-hemisphere basin for the cases without or with the throughflow.

Note that for the case with symmetric forcing, our formulation is reduced to the solution discussed by Pedlosky (1996), with the equator as the separating line of these two branches; that is, $y_{sep} = 0$.

The boundary value problem consists of two sets of ordinary differential equation systems. Each set is subjected to the matching boundary conditions at the matching latitude y_m; these two solutions match along a free boundary y_{sep}, which is part of the solution. Across this matching boundary, the upper- and lower-layer thicknesses are continuous, as required. However, the zonal velocity may be discontinuous because the Bernoulli function from the two hemispheres can be different. A solution with $B_0^s = 1.25B_0^n$ is shown in Figs. 2 and 3.

The solution is very similar to the case with a symmetric forcing, and it is slightly asymmetric with respect to the equator (Fig. 2). The thermocline depth resembles the gross structure of the equatorial thermocline observed in the oceans. The most outstanding feature of this solution is the discontinuity of the zonal velocity across the separating streamline, and this discontinuity can be seen clearly in the meridional sections shown in Fig. 3.

The western boundary currents from the two hemispheres meet near the equator and form the eastward-moving Equatorial Undercurrent. Due to the difference in the Bernoulli head, the zonal velocity is discontinuous across the separating streamline, as shown in Fig. 3a. As the undercurrent moves eastward, the zonal velocity core becomes stronger, and the separating streamline moves slightly toward the equator, as shown by the line labeled as y_{sep} in lower part of Fig. 3a.

The meridional structure of the undercurrent can be represented by the meridional section taken along the western boundary, as shown in Figs. 3b, 3c, and 3d. As required by the matching boundary condition, the thermocline depth is continuous (Fig. 3d). However, both the zonal velocity and the Bernoulli function are discontinuous across the separation line (Figs. 3b and 3c).

It is important to note that this ideal-fluid solution may not be very stable. In fact, the solution consists of a rather narrow band north of the equator, where a patch of negative potential vorticity originating from the Southern Hemisphere is adjacent to the positive potential vorticity in the Northern Hemisphere (Fig. 4a). The coexistence of potential vorticity with opposite signs indicates that symmetric instability may occur and thus modify the solution.

Second, it is readily shown that the zonal velocity profile satisfies the sufficient condition for barotropic instability. The barotropic instability is likely to smooth out the velocity cusp near the equator. Even for the hemispherical symmetric solution first obtained by Pedlosky (1987), it is readily shown that the zonal profile

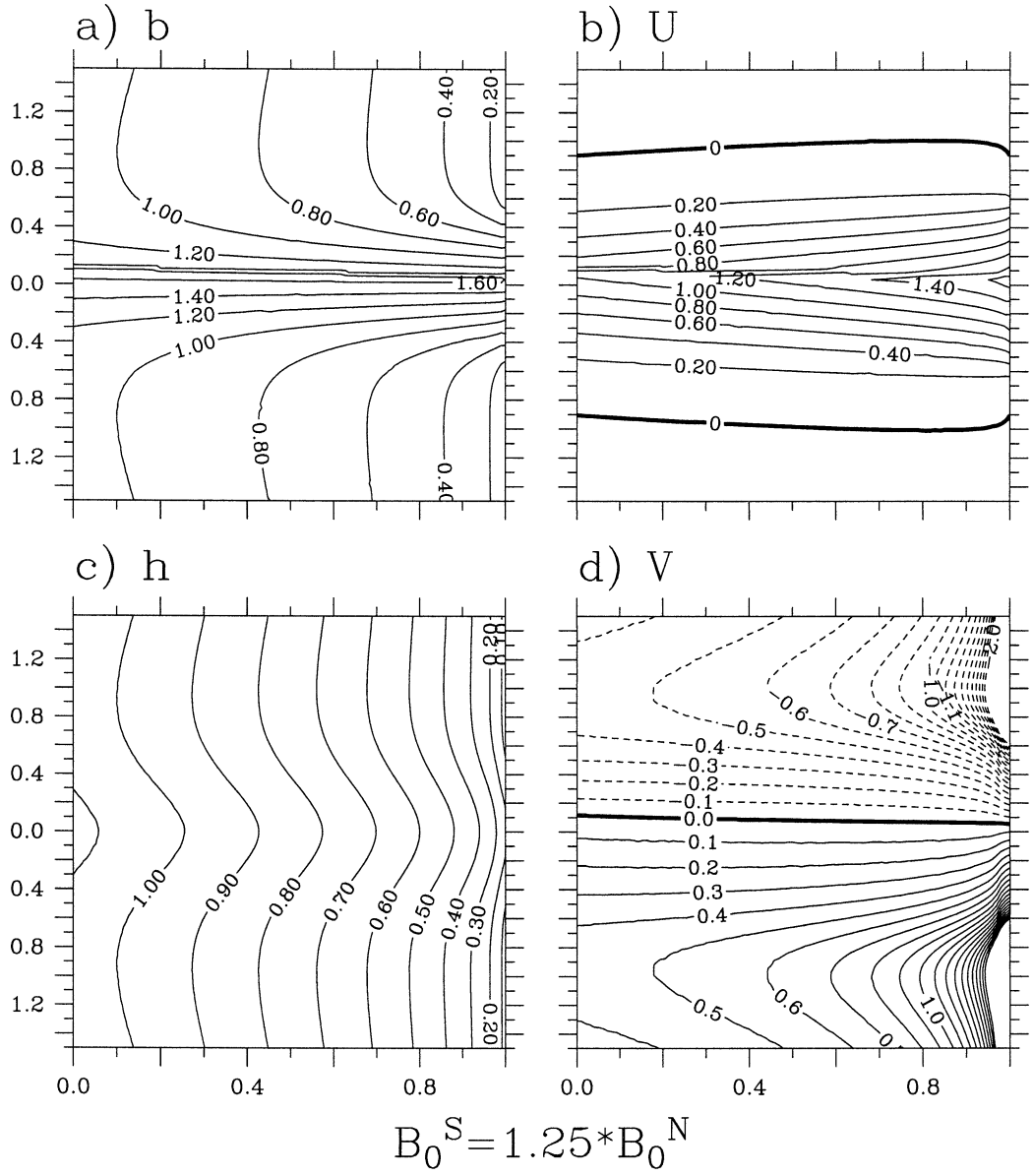

FIG. 2. Structure of the Equatorial Undercurrent in a two-hemisphere ocean, under the asymmetric forcing, $B_0^S = 1.25B_0^n$, plotted in nondimensional x, y coordinates: (a) the Bernoulli function, (b) the zonal velocity, (c) the thermocline depth, and (d) the meridional velocity.

of the solution satisfies the necessary condition for barotropic instability.

The fact that symmetric instability may arise from the hemispheric asymmetric solution may also not be a significant deficiency. To some extent, it may be a realistic property. It was suggested recently by Hua et al. (1997) that the observed equatorial mean circulation may marginally satisfy the condition for symmetric instability. Using a numerical model, they further demonstrated that for a basic state flow with this kind of instability, the nonlinear equilibrated state of the equatorial ocean circulation exhibits some secondary flows that resemble the observed multiple equatorial jets underneath the Equatorial Undercurrent (Firing 1987).

3. Application to the Pacific Ocean

a. Evidence of off-equator shift of the Equatorial Undercurrent core

Direct field measurements also indicated the asymmetrical nature of the zonal velocity profile in the Equatorial Undercurrent. Hayes (1982) studied the zonal geostrophic velocity profile at two sections (110° and

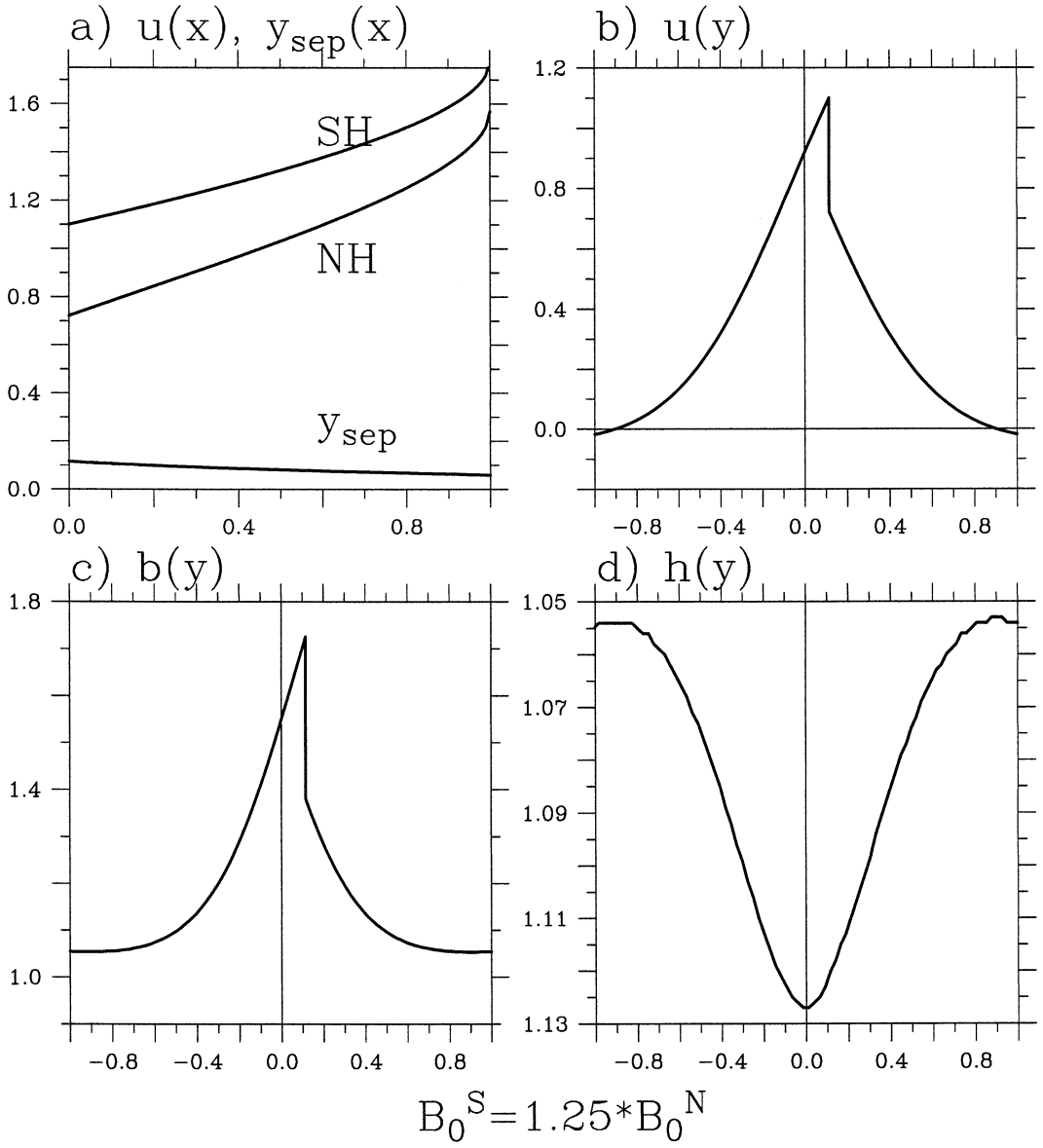

FIG. 3. The zonal and meridional structure of the undercurrent. (a) The zonal variation of the zonal velocity along the matching streamline, plotted in a nondimensional x coordinate. Here SH (NH) indicates the water particle originating from the Southern (Northern) Hemisphere, and y_{sep} indicates the zonal variation of the separation point. (b) The zonal velocity at the western boundary, plotted in nondimensional y coordinates; (c) the Bernoulli function along the western boundary, plotted in nondimensional y coordinates; and (d) the thermocline depth along the western boundary, plotted in nondimensional y coordinates.

125°W) in the eastern equatorial Pacific. Geostrophic velocity calculated from hydrographic data is consistent with that obtained from the free-fall acoustically tracked velocimeter (TOPS). The geostrophic velocity south of the equator (at 0.5° and 1°S) was clearly stronger than that north of the equator. Wyrtki and Kilonsky (1984) calculated the geostrophic zonal velocity from the data collected during the Hawaii–Tahiti Shuttle Experiment, which was carried out along 150°, 153°, and 150°W. Their results showed that the center of the Equatorial Undercurrent is located at 0.5°S. However, Lukas and Firing (1984) used profiling current meter data and density data and shown that both the (equatorial) geostrophic and measured Equatorial Undercurrent were centered on the equator.

However, in the western part of the Pacific equatorial ocean, the core of the undercurrent is located north of the equator. Tsuchiya et al. (1989) made a detailed analysis of the water mass properties collected during the Western Equatorial Pacific Ocean Circulation Study

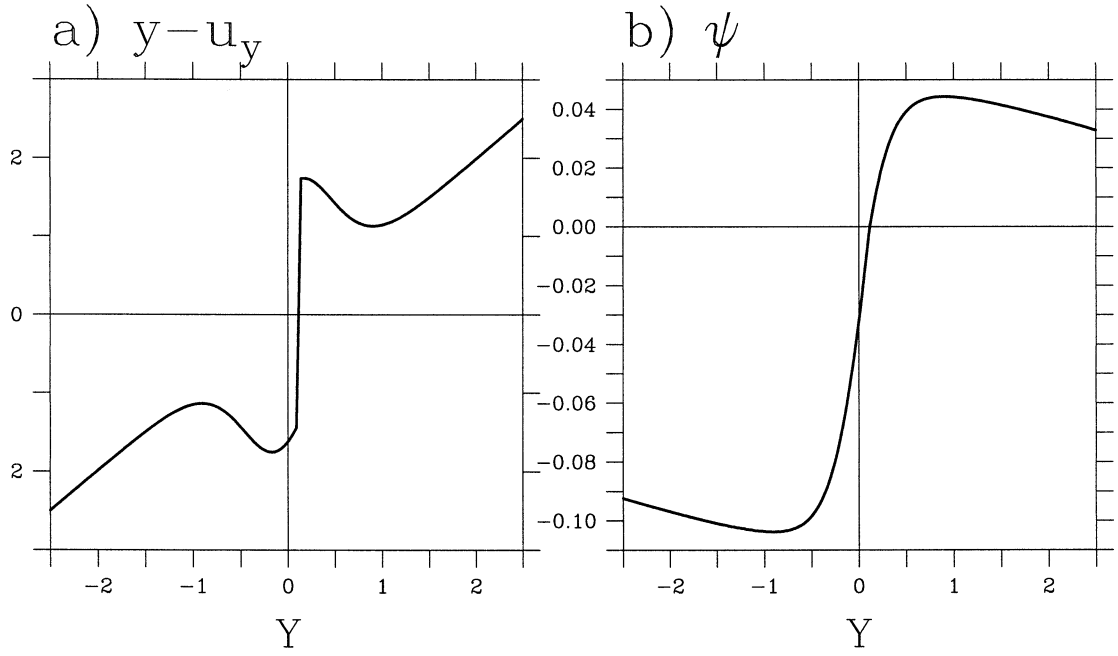

FIG. 4. The meridional profile of (a) the total vorticity and (b) the streamfunction at the western boundary.

(WEPOCS). Their analysis clearly showed that the major portion of the water in the Equatorial Undercurrent at its beginning north of Papua New Guinea is supplied from the south by a narrow western boundary undercurrent (New Guinea Coastal Undercurrent). In fact, the water mass north of the equator can be traced back to its source in the south.

Gouriou and Toole (1993) analyzed the mean circulation in the western equatorial Pacific Ocean. Their Fig. 8b clearly showed there is a patch of negative potential vorticity north of the equator, adjacent to the positive potential vorticity in the environment. Such a patch of negative potential vorticity must come from the Southern Hemisphere.

Joyce (1988) argued that the wind stress on the equatorial ocean can force a cross-equatorial flow in the upper ocean. By applying a generalized Sverdrup relation to the equatorial oceans, he inferred that there is a southward cross-equatorial flow in the eastern equatorial Pacific Ocean and a northward cross-equatorial flow in the western equatorial Pacific Ocean. His calculation, however, did not include the contribution due to the relative vorticity term nor the connection with the western boundary currents. Therefore, his analysis may provide an explanation for the southward shift of the Equatorial Undercurrent farther east.

The total mass flux going through the western boundary at the beginning of the undercurrent can be estimated from the lower-layer streamfunction profile shown in Fig. 4b. For example, the mass flux from the Southern and Northern Hemispheres is about 0.1 and 0.05 in nondimensional units. For the Pacific Ocean, the scale of the streamfunction is about 225 Sv; thus, the mass flux contribution from the western boundary currents is about 23 and 11 Sv. The cross-equatorial flux ψ_0 is about 0.03 nondimensional unit, which corresponds to about 6 Sv in dimensional units. Tsuchiya et al. (1989) estimated that the mass flux of 5 Sv is fed to the eastward interior circulation between 3°S and the equator. If there were no Indonesian Throughflow, this would be the mass flux fed to the undercurrent. This flux rate is rather close to the 6 Sv estimated in the discussion above.

b. Determination of the cross-equatorial flow in the source regime of the undercurrent

The dynamic factor that controls the position of the separating streamline is the strength of the Bernoulli function at the latitude of the western boundary bifurcation. In reality, the bifurcation of the western boundary is a complicated three-dimensional phenomenon, which is determined by many dynamic factors, such as the large-scale forcing fields and the resulting pressure field, the shape of the coastline, bottom topography, and eddies. In this study, we will assume that the separation latitude can be approximately determined by the barotropic circulation, which can be quite easy to calculate from the wind stress data. Thus, a barotropic bifurcation latitude may provide a simple and useful first step to this complicated problem.

Note that in our conceptual model the bifurcation latitudes are higher than the outcropping latitudes, so in the following discussion, there is a single moving layer below the Ekman layer. The Bernoulli head is determined by the depth of the thermocline, which can

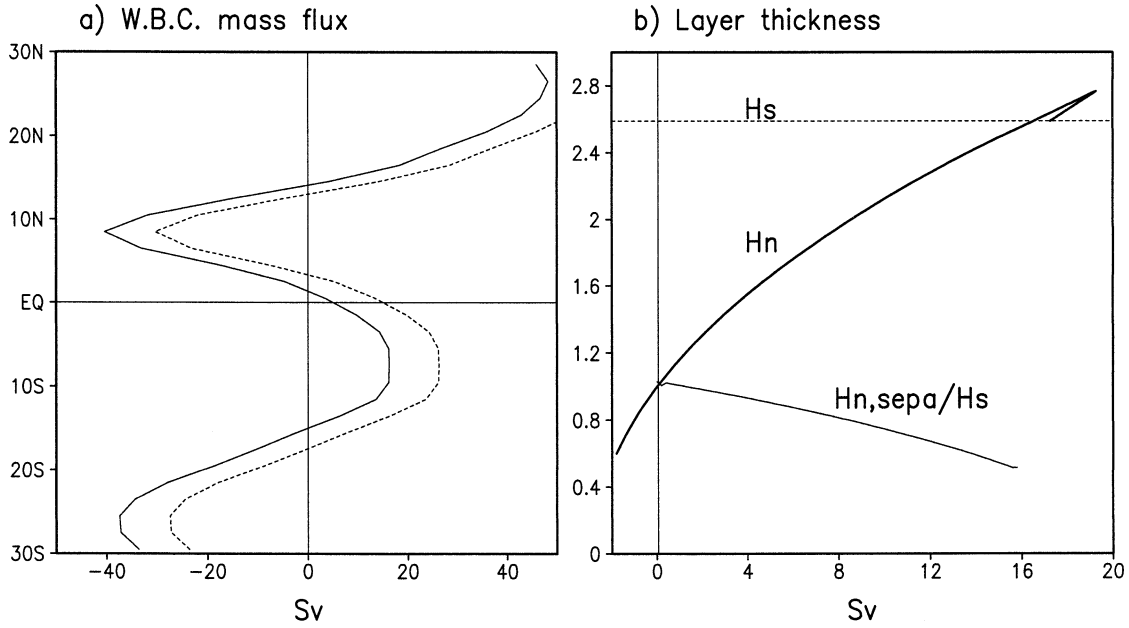

FIG. 5. Determination of the ratio of the thermocline depth (Bernoulli head) of equatorward western boundary flow. (a) The volume flux in the western boundary current in the Pacific Ocean (Sv). The solid lines indicate the case without throughflow and the dashed line is for the case with a 10-Sv throughflow; (b) the depth of the thermocline at the separation latitude, H_S for the Southern Hemisphere, including a correction due to the additional mass flux associated with the throughflow; H_N depicts the thermocline depth as a function of the geostrophic volume flux along the section at the separation latitude (14.5°N), in units of 100 m. The thin line $H_{N,sepa}/H_S$ depicts the ratio of thermocline depth.

be inferred from a simple reduced-gravity model for this domain.

The total poleward Ekman flux across a latitudinal section is

$$M_E = -\int_0^L \frac{\tau^x}{f\rho_0}\,dx, \tag{19}$$

and the poleward geostrophic flux is

$$M_G = \int_0^L \frac{fw_e}{\beta}\,dx, \tag{20}$$

where w_E is the Ekman pumping velocity calculated from wind stress [Eq. (3)]. Note that M_E is positive (negative) for the Northern (Southern) Hemisphere, and M_G is negative (positive) for the Northern (Southern) Hemisphere.

The total meridional mass flux involved in the wind-driven gyre across a latitudinal section of the basin interior is the sum of these two fluxes, that is, $M_{\rm Sv} = M_E + M_G$. The return flow into the western boundary is $-M_{\rm Sv}$. For a simple reduced-gravity model, the bifurcation latitude of the western boundary current is the latitude where $M_{\rm Sv}$ vanishes, and it can be found out from the wind stress distribution in the basin. From the Florida State University (FSU) wind stress data collected over the equatorial Pacific Ocean for the period 1961–99, this gives the separation latitude as 14.5°N for the North Pacific and 15°S for the South Pacific (Fig. 5a). These locations are close to the bifurcation points estimated from a numerical model (e.g., Huang and Liu 1999).

For a given amount of wind stress, the depth of the main thermocline can be calculated using a simple reduced-gravity model. The corresponding Bernoulli function can be calculated according to the definition: $B = g'H$, where g' is the reduced gravity, chosen as $g' = 2$ cm s^{-2} for the Pacific, and H is the depth of the main thermocline.

This simple approach is, however, unsatisfactory because over the subtropical and Tropical latitudes the zonally integrated wind stress curl is slightly larger in the Northern Hemisphere and the corresponding Bernoulli head in the Northern Hemisphere is larger than that in the Southern Hemisphere (see Fig. 5b). In this figure, the dashed line indicates the thermocline depth at the western boundary at the latitude of separation (15°S). The thick solid line depicts how the thermocline depth varies as a function of the geostrophic transport along the latitude of separation in the Northern Hemisphere. It is clear that at the separation latitudes thermocline depth in the Northern Hemisphere is larger than in the Southern Hemisphere.

As a result, this simple approach would lead to a conclusion that water from the Northern Hemisphere western boundary should invade the Southern Hemisphere. However, observations indicate that most water forming the Equatorial Undercurrent does come from the south, as discussed above. Thus, in order to have

the water from the Southern Hemisphere overshoot the equator, another mechanism is needed. A strong contender is the Indonesian Throughflow. With the throughflow, the western boundary current system changes and the source of the undercurrent also change accordingly, as shown schematically in Fig. 1b.

Australia can be treated as a big island, so the simple island rule can apply and yield a circulation around the island that is a simple function of the wind stress. The island rule has been discussed in many papers, and the most important physical mechanisms associated with this rule have been discussed throughly by Godfrey (1989, 1996).

Although the island rule gives a simple recipe for the throughflow, the actual mass flux of the Indonesian Throughflow depends on many physical processes. For example, Godfrey et al. (1993) analyzed the circulation around Australia, using both analytical formula and numerical models. A straightforward application of the island rule gives rise to a circulation around the island, with a volume flux of 17 Sv for the Indonesian Throughflow that comes from the Southern Pacific. However, numerical simulation based on general circulation models and observation indicate that the volume flux of the Indonesian Throughflow is about 10 Sv. Most importantly, the water in the throughflow carries properties that clearly belong to the North Pacific. The exact pathway of the throughflow water is beyond the scope of this study.

In our purely inertial model, water from the Southern Hemisphere could not penetrate into the Northern Hemisphere or feed the throughflow without changing sign of the potential vorticity. The western boundary current from the Southern Hemisphere has to go through the undercurrent first. Over the eastward trajectory this mass flux upwells into the Ekman layer and then moves poleward in the form of Ekman transport. Thus, mass flux from the Southern Hemisphere becomes part of the Sverdrup mass flux in the ocean interior of the Northern Hemisphere. Within the simple ideal-fluid formulation of our model the only option is to assume that the throughflow is fed from the western boundary from the Northern Hemisphere; hence, we will simply assume that, indeed, about 10 Sv of water leaves the basin and forms the Indonesian Throughflow.

With the existence of an island, the separation latitude and the Bernoulli head of the effective western boundary current feeding the Equatorial Undercurrent are modified as follows.

In the Northern Hemisphere, the separation latitude is not affected by the throughflow; mass flux in the western boundary current is zero at the separation latitude. However, the effective western boundary current that feeds the undercurrent actually comes from the ocean interior. To find the Bernoulli head of this western boundary layer, one has to search eastward, starting from the western boundary at the separation latitude, for a place where the equatorward flux, integrated from the eastern boundary, satisfies

$$\psi^{\text{North}}_{\text{effe,wbc}} = \psi_{\text{wbc}} - \Delta\psi, \tag{21}$$

where $\psi_{\text{wbc}} = -M_{\text{Sv}}$ is the Sverdrup flux at the outer edge of the western boundary; $\Delta\psi = 10$ Sv is the volumetric contribution to the throughflow from the wind-driven circulation.

In the Southern Hemisphere, the separation latitude is now determined by the constraint that the total mass flux in the western boundary layer,

$$\psi^{\text{South}}_{\text{effe,wbc}} = -M_{\text{Sv}} + \Delta\psi, \tag{22}$$

vanishes. Because of the northward mass flux of the flow around the island, the separation latitude of the western boundary current in the Southern Hemisphere is moved southward to 17°S, as shown by the dashed line in Fig. 5a. Note that in the existance of the throughflow the western boundary flux should be the combination of the solid line north of 10°N and the dashed line south of 10°S.

In addition, the additional geostrophic mass associated with the throughflow reduces the pressure head along the western boundary. Note that we assume the western boundary is a frictional boundary current, so the contribution of the kinetic energy term to the pressure head is negligible. Therefore, the thermocline depth and the Bernoulli function are the same, except for a constant coefficient.

As a result, the thermocline depth of the effective western boundary current is

$$H_{\text{s,eff}} = \sqrt{H_s^2 - \frac{2f\Delta\psi}{g'}}. \tag{23}$$

Using the FSU wind stress, without the throughflow the separation latitude would be 15°S, and the corresponding thermocline depth would be $H_s^0 = 240$ m. With the throughflow, the separation latitude is moved to 18°S, and the thermocline depth corresponding to the western boundary current associated with the interior Sverdrup flow, $H_s = 335$ m. Including the northward mass flux of 10 Sv associated with the throughflow, the thermocline depth of the effective western boundary is reduced to 258 m. As depicted by the thin solid line labeled as $H_{N,\text{sepa}}/H_S$, the ratio of the thermocline depth (or the Bernoulli head) is about 0.74 for a mass flux of the throughflow $\Delta\psi = 10$ Sv. Therefore, the western boundary current from the Southern Hemisphere overshoots the equator and the water in the western part of the undercurrent comes primarily from the Southern Hemisphere.

4. Application to the Atlantic Ocean

The situation in the Atlantic is quite different. There is no mass flux cross the western boundary, so the argument presented above does not apply. However, it is

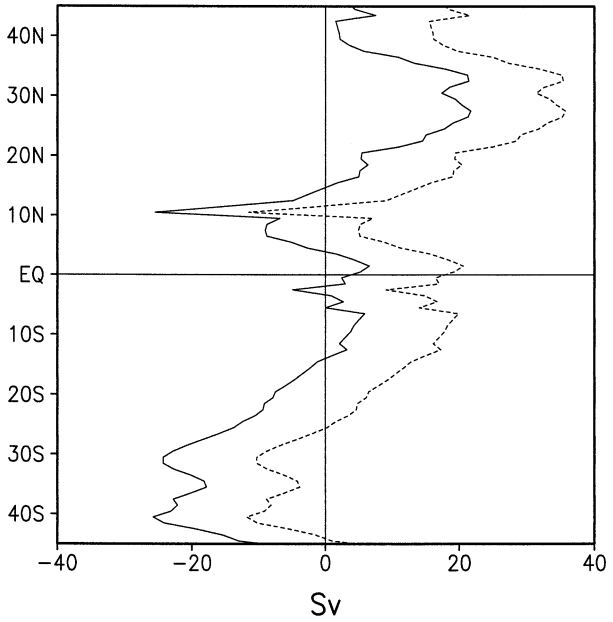

FIG. 6. Northward volume flux of the western boundary currents in the Atlantic, without the thermohaline component (solid line) and with the thermohaline component (dashed line).

well known that thermohaline circulation in the Atlantic basin is very strong. As a result, there is a cross-equator volume transport of 14 Sv (Schmitz 1996). If there is no thermohaline contribution, the western boundary current in the South Atlantic bifurcates around 14.5°S, while the western boundary current in the Northern Hemisphere bifurcates around 12°N as indicated by the heavy line in Fig. 6 [based on the wind stress data of da Silva et al. (1994)]. Thus, our simple model discussed in section 2 would apply. However, with the thermohaline component added the western boundary current in the Southern Hemisphere bifurcates around 22°S, while the western boundary current in the Northern Hemisphere is poleward at all latitudes, with an exception at 10°N. Thus, adding the thermohaline component to our argument, the wind-driven circulation in the North Atlantic does not seem to contribute to the Equatorial Undercurrent in the Atlantic basin. Consequently, the Equatorial Undercurrent in the Atlantic is fed from the Southern Hemisphere only. This is consistent with the observations. In fact, there are three undercurrents in the Atlantic basin: the South Equatorial Undercurrent, the Equatorial Undercurrent, and the North Equatorial Undercurrent, and water mass in all these currents come from the Southern Hemisphere (Bourles et al. 1999). In other words, the structure of the Equatorial Undercurrent in the Atlantic is also asymmetric with respect to the equator because all water in these currents come from the Southern Hemisphere.

Acknowledgments. Reviewers' critical comments helped to clear up the connection between the undercurrent and the throughflow. This study was carried out during a sabbatical visit of FFJ to Woods Hole Oceanographic Institution, arranged through the NOAA CICOR visiting scholar program. RXH is supported by NOAA through Grant NA36GP0460 and the National Science Foundation through Grant OCE-0094807 to Woods Hole Oceanographic Institution. FFJ is supported by a NSF grant through University of Hawaii.

REFERENCES

Anderson, D. L. T., and D. W. Moore, 1979: Cross-equatorial inertial jets with special relevance to very remote forcing of the Somali current. *Deep-Sea Res.,* **26,** 1–22.

Blanke, B., and S. Raynaud, 1997: Kinematics of the Pacific Equatorial Undercurrent: An Eulerian and Lagrangian approach from GCM results. *J. Phys. Oceanogr.,* **27,** 1038–1053.

Bourles, B., R. L. Molinari, E. Johns, W. D. Wilson, and K. D. Leaman, 1999: A synoptic study of the upper layer circulation in the western tropical North Atlantic. *J. Geophys. Res.,* **104,** 1361–1376.

da Silva, A. M., C. C. Young, and S. Levitus, 1994: *Algorithms and Procedures.* Vol. 1, *Atlas of Surface Marine Data 1994,* NOAA Atlas NESDIS, 83 pp.

Edwards, C. A., and J. Pedlosky, 1998: Dynamics of nonlinear cross-equatorial flow. Part I: Potential vorticity transformation. *J. Phys. Oceanogr.,* **28,** 2382–2406.

Fine, R. A., W. H. Peterson, and H. G. Ostlund, 1987: The penetration of tritium into the tropical Pacific. *J. Phys. Oceanogr.,* **17,** 553–564.

Firing, E., 1987: Deep zonal currents in the central equatorial Pacific. *J. Mar. Res.,* **45,** 791–812.

Fratantoni, D. M., W. E. Johns, T. L. Townsend, and H. E. Hurlburt, 2000: Low-latitude circulation and mass transport pathways in a model of the tropical Atlantic Ocean. *J. Phys. Oceanogr.,* **30,** 1944–1966.

Godfrey, J. S., 1989: A Sverdrup model of the depth-integrated flow for the world ocean allowing for island circulations. *Geophys. Astrophys. Fluid Dyn.,* **45,** 89–112.

——, 1996: The effect of the Indonesian throughflow on ocean circulation and heat exchange with the atmosphere: A review. *J. Geophys. Res.,* **101,** 12 217–12 237.

——, A. C. Hirst, and J. Wilkin, 1993: Why does the Indonesian Throughflow appear to originate from the North Pacific? *J. Phys. Oceanogr.,* **23,** 1087–1098.

Gouriou, Y., and J. Toole, 1993: Mean circulation of the upper layers of the western equatorial Pacific Ocean. *J. Geophys., Res.,* **98** (C12), 22 495–22 520.

Hayes, S. P., 1982: A comparison of geostrophic and measured velocity in the Equatorial Undercurrent. *J. Mar. Res.,* **40** (Suppl.), 219–229.

Hua, B. L., D. Moore, and S. Le Gentil, 1997: Inertial nonlinear equilibration of the equatorial flows. *J. Fluid Mech.,* **331,** 345–371.

Huang, B., and Z. Liu, 1999: Pacific subtropical–tropical thermocline water exchange in the National Centers for Environmental Prediction ocean model. *J. Geophys. Res.,* **104** (C5), 11 065–11 076.

Huang, R. X., and J. Pedlosky, 2000: Climate variability of the equatorial thermocline inferred from a two-layered model of the ventilated thermocline. *J. Phys. Oceanogr.,* **30,** 2610–2626.

——, and Q. Wang, 2001: Interior communication window and the structure of the equatorial thermocline. *J. Phys. Oceanogr.,* **31,** 3538–3550.

Johnson, G. C., and M. J. McPhaden, 1999: Interior pycnocline flow from the subtropical to the equatorial Pacific Ocean. *J. Phys. Oceanogr.,* **29,** 3073–3089.

Joyce, T. M., 1988: On wind-driven cross-equatorial flow in the Pacific Ocean. *J. Phys. Oceanogr.,* **18,** 19–24.

Killworth, P. D., 1991: Cross-equatorial geostrophic adjustment. *J. Phys. Oceanogr.,* **21,** 1581–1601.

Liu, Z., 1994: A simple model of the mass exchange between the subtropical and tropical ocean. *J. Phys. Oceanogr.,* **24,** 1153–1165.

Lu, P., and J. P. McCreary, 1995: Influence of the ITCZ on the flow of the thermocline water from the subtropical to the equatorial Pacific Ocean. *J. Phys. Oceanogr.,* **25,** 3076–3088.

——, ——, and B. A. Klinger, 1998: Meridional circulation cells and the source waters of the Pacific Equatorial Undercurrent. *J. Phys. Oceanogr.,* **28,** 62–84.

Lukas, R., and E. Firing, 1984: The geostrophic balance of the Pacific Equatorial Undercurrent. *Deep-Sea Res.,* **31,** 61–66.

Luyten, J. R., J. Pedlosky, and H. Stommel, 1983: The ventilated thermocline. *J. Phys. Oceanogr.,* **13,** 292–309.

McCreary, J. P., and P. Lu, 1994: Interaction between the subtropical and equatorial ocean circulation: The subtropical cell. *J. Phys. Oceanogr.,* **24,** 466–497.

McPhaden, M. J., and R. A. Fine, 1988: A dynamical interpretation of the tritium maximum in the central equatorial Pacific. *J. Phys. Oceanogr.,* **18,** 1454–1457.

Pedlosky, J., 1987: An inertial theory of the Equatorial Undercurrent. *J. Phys. Oceanogr.,* **17,** 1978–1985.

——, 1996: *Ocean Circulation Theory.* Springer-Verlag, 453 pp.

Schmitz, W. J., Jr., 1996: On the world ocean circulation, Vol. II: The Pacific and Indian Ocean/A global update. Woods Hole Oceanographic Institution Tech. Rep. WHOI-96-08, 241 pp.

Tsuchiya, M., R. Lukas, R. A. Fine, E. Firing, and E. Lindstrom, 1989: Source waters of the Pacific Equatorial Undercurrent. *Progress in Oceanography,* Vol. 23, Pergamon, 101–147.

Wijffels, S., 1993: Exchanges between hemisphere and gyres: A direct approach to the mean circulation of the equatorial Pacific. Ph.D. thesis, MIT/WHOI, 272 pp.

Wyrtki, K., and B. Kilonsky, 1984: Mean water and current structure during the Hawaii–Tahiti Shuttle Experiment. *J. Phys. Oceanogr.,* **14,** 242–254.